Composition as a Means to Control Morphology and Properties of Epoxy Based Dual-Phase Structural Electrolytes

Natasha Shirshova[*1†], *Alexander Bismarck*[1,2], *Emile S. Greenhalgh*[3], *Patrik Johansson*[4‡], *Gerhard Kalinka*[5], *Maciej J. Marczewski*[4], *Milo S.P. Shaffer*[6], *Malte Wienrich*[5]

[1]Department of Chemical Engineering, Polymer and Composite Engineering (PaCE) Group, Imperial College London, South Kensington Campus, London, SW7 2AZ, U.K.

[2]Polymer and Composite Engineering (PaCE) Group, Institute of Materials Chemistry & Research, Faculty of Chemistry, University of Vienna, Währingstr.42, A-1090 Vienna.

[3]The Composites Centre, Imperial College London, South Kensington Campus, London, SW7 2AZ, U.K.

[4]Department of Applied Physics, Chalmers University of Technology, SE-41296 Göteborg, Sweden.

[5]BAM Federal Institute for Materials Research and Testing, Unter den Eichen 87, D-12205, Berlin, Germany.

† School of Engineering and Computing Sciences, Durham University, Lower Mountjoy, Durham, DH1 3LE, U.K.

‡ Visiting Professor at LRCS/CNRS UMR7314, Université de Picardie Jules Verne, 33 rue Saint Leu, 80039 Amiens, France

[6]Department of Chemistry, Imperial College London, South Kensington Campus, London, SW7 2AZ, U.K.

ABSTRACT

Structural electrolytes were prepared using a fully formulated commercially available high performance epoxy resin (MTM57) and an ionic liquid based electrolyte: lithium bis(trifluoromethylsulfonyl)imide (LiTFSI) dissolved in 1-ethyl-3-methylimidazolium bis(trifluoromethylsulfonyl)imide (EMIM-TFSI). Through a systematic study, the composition of the formulations was found to have a greater effect than the curing temperature on the morphology and properties of the resulting structural electrolytes. The presence of lithium salt is essential to form a structurally homogeneous electrolyte. Bicontinuous morphologies containing continuous (coarse) epoxy networks surrounded by connected spherical epoxy nodules were obtained with different length scales upon varying the lithium salt concentration. Increasing the LiTFSI concentration improved the miscibility of MTM57 with the electrolyte and decreased the characteristic length scale of the resulting bicontinuous microstructure. The properties of the structural electrolytes correlated with the morphology, showing increased Young's modulus and decreased ionic conductivity with increasing lithium salt concentration. The miscibility of the epoxy system with the electrolyte was also improved by substitution of EMIM-TFSI with an equal weight of an aprotic organic solvent, propylene carbonate (PC); however, the window of PC concentrations which resulted in structural electrolytes with bicontinuous microstructures was very narrow; at PC concentrations above 1 wt.%, gel-like polymers with no permanent mesoporosity were obtained.

KEYWORDS: microstructure; mechanical properties; ionic conductivity; multifunctional materials

INTRODUCTION

Research on energy storage device components relies both on the modification of existing materials,[1-4] and the development of new materials for electrodes, separators and electrolytes.[3, 5-9] Developing electrolytes with significant load-bearing mechanical performance, termed structural electrolytes, offers potential benefits, such as improved safety and robustness,[6, 10, 11] and new opportunities for multifunctional energy storage devices.[12] The most promising route to combining high ionic conductivity with substantial mechanical properties is to create bicontinuous structures in which one phase provides mechanical strength and the other ion conduction; examples can be found in the literature based on different polymers and processes for microstructure formation.[9, 13-17] Routes have been developed using both templating, sol-gel[15] and high internal phase emulsion approaches,[9] as well as non-templating, temperature or polymerization induced phase separation,[14, 16, 17] methods. Unfortunately, any direct comparison of techniques is difficult due to the different polymers and electrolytes used. Nevertheless, electrolytes obtained by the modification of epoxy/amine systems seem to be the most promising in terms of achieved levels of multifunctionality:[10] the extent to which ionic conductivity can be improved relative to the associated decrease in mechanical performance compared to the purely structural epoxy resin.[18, 19] The interest in epoxy/amine systems is also driven by the excellent set of specific properties of the cured resins, including excellent mechanical properties as well as thermal and chemical stability. It has been shown in the literature[10, 18] that the properties of the final structural electrolytes are affected by the microstructure of the polymer phase. As epoxies have the ability to form bicontinuous structures *via* polymerization induced phase separation,[20-23] this approach has been used to produce porous monoliths for chromatography and biomedical applications.[24] Mixing epoxy resin with other compounds does not, however,

always result in a bicontinuous structure and there is no simple method to predict the phase behavior. Depending on composition and curing temperature, monoliths with different microstructures may be obtained, ranging from connected nodules, to 3D-bicontinuous networks, or any (multiphase) combination thereof.[25-27] Initial solubility, type, molecular weight, amount of the second phase / porogen, as well as the epoxy/amine ratio and the curing temperature must all be considered. As a pertinent example,[20] the morphology of blends of diglycidyl ether of bisphenol A (DGEBA) / bis (4-aminocyclohexyl)methane with polyethylene glycol (PEG) was transformed from a nodular microstructure into a 3D-bicontinuous network when the curing temperature was raised from 90°C to 130°C. For blends of DGEBA/diethyltoluenediamine with a liquid rubber, carboxyl terminated poly(2-ethyl hexyl acrylate)[28] and DGEBA/ 2,2-bis(4-amino-cyclohexyl)methane with cyclohexane[29], however, the curing temperature had no effect on the final microstructure. Upon mixing epoxy with carboxyl terminated poly(2-ethyl hexyl acrylate) in cyclohexane, the microstructure comprised droplets of the second component randomly dispersed in the epoxy bulk.

There is no simple relationship between molecular weight and the microstructure formed. Taking epoxy/PEG blends as an example, it might be expected that increasing the molecular weight of the PEG would increase miscibility of PEG/epoxy system due to the proportionate reduction in terminal hydroxyls and hence decreased polarity of the PEG. Varying the content and molecular weight (from 150 to 400 g/mol) of PEG in an epoxy/amine system generated materials with wide range of microstructures, from gels to fused nodules, 3D-bicontinuous networks, and combinations thereof. 3D-bicontinuous microstructures were formed in a wide range of concentrations when PEG200 was blended with epoxy/amine. [20] However, no phase separation was reported [30] for systems using PEG with a molecular weight below 800g/mol.

There are some previous examples of epoxy blends with ionic liquids (ILs),[18, 31-33] mainly considering the use of ILs as curing agents, while the information about the resulting microstructures is surprisingly limited. ILs not only possess a wide range of remarkable properties, including high thermal stability, negligible vapor pressure, high ionic conductivity, broad liquid range, and excellent heat transfer properties,[34-39] but also great versatility in applications. As well as the possibilities for tuning the IL properties, by varying the cation and anion[34, 40], the performance of the epoxy can be modulated, since many ILs can be used as curing agents.[31, 33, 41-44] In addition, the properties/structure (morphology) of the epoxy/IL blends and resulting cured epoxies can be adjusted, for example to improve wear and scratch resistance,[32, 33] thermal stability[44] or ion conduction.[10, 18]

In an earlier study, we described a strong effect of the morphology on the properties of electrolytes based on a blend of an epoxy/amine system and a lithium salt doped IL[10]; the conclusion was that a relatively coarse bicontinuous structure is the most promising for structural electrochemical applications. Here, we further tune the morphology to optimize the desirable combination of ionic conductivity and mechanical performance, using commercial epoxy resin and IL based electrolytes. The choice of the fully formulated commercially available epoxy, despite its complex composition, was primarily determined by its excellent mechanical performance and the possibility of straightforward scale up of any successful material. The effects of curing temperature and electrolyte composition on the morphology and properties will be discussed. The presented data also contribute to a better understanding of structure-property relationships of epoxy and IL based blends.

EXPERIMENTAL

Materials

A fully formulated epoxy-based resin was used; MTM57 (Cytec Industrial Materials) is a white paste resin with a viscosity of 4835 Pa·s typically used for composite manufacturing *via* the prepreg route, and the system contains epoxy and amine group(s) as the primary chemistry. 1-Ethyl-3-methylimidazolium bis(trifluoromethylsulfonyl)imide (EMIM-TFSI, 99%, Iolitec), the corresponding lithium salt (LiTFSI, puriss., ≥99.0% (^{19}F-NMR, Aldrich)) and propylene carbonate (PC, Aldrich) were stored in a dry cabinet (over P_2O_5). All chemicals, including solvents for extraction and purification were used as received.

Preparation of epoxy resin based electrolytes

Prepared formulations were cured in two different shapes: monoliths (dxh = 12x60 mm) and thin (2-3mm) plaques. High density polyethylene cylindrical shaped moulds were used to manufacture the monoliths and two glass slides treated with a mould release agent (Frekote 700NC, LOCTITE), separated using a silicone rod spacer and held together using bulldog clips, were used for manufacturing thin (2-3 mm) plaques.

The general preparation procedure can be described as follows: LiTFSI was dissolved in EMIM–TFSI, in an oven at 50°C. The prepared electrolyte solution was then added to the epoxy resin. For the preparation of structural electrolytes containing PC, the composition of the initial electrolyte solution was adjusted accordingly by replacing the required amount of IL by PC. The MTM57 to EMIM-TFSI (or EMIM-TFSI+PC) ratio was kept constant at 50:50 wt.% (50MTM57) following earlier findings[10]. A jar containing the components was placed for 5 min in a fan convection oven (Carbolite PF30) at 75°C and then the components were mixed using a speedmixer TM DAC 150FVZ-K until a mixture with uniform consistency was obtained, usually after 4 min blending at 3000 rpm. Subsequently, the mixture was transferred into a preheated (75°C) mould and cured using the following cycle: ramp to 120°C

(if not specified otherwise) at 0.5°C/min; dwell at 120°C for 60 min (if not specified otherwise); ramp to room temperature at 3°C/min. The compositions of the studied formulations are summarized in **Table 1** and **2**. After removal from the oven, all samples were vacuum-bagged and stored in a dry cabinet.

Table 1. Compositions of epoxy resin based formulations MTM57:EMIM-TFSI 50:50 wt.% with different concentrations of LiTFSI .

Sample	EMIM-TFSI +LiTFSI [g]	LiTFSI [g]	[LiTFSI] [mol/l]
0.5M_50MTM57	16.382	1.917	0.5
1.0M_50MTM57	17.765	3.835	1.0
1.5M_50MTM57	19.147	5.752	1.5
2.0M_50MTM57	20.529	7.670	2.0
2.3M_50MTM57	21.359	8.844	2.3
2.5M_50MTM57	21.912	9.587	2.5
3.0M_50MTM57	23.294	11.505	3.0
3.5M_50MTM57	24.677	13.422	3.5
4.0M_50MTM57	26.056	15.334	4.0
4.6M_50MTM57	27.712	17.648	4.6

*The concentration of LiTFSI was calculated taking into account only the volume of EMIM-TFSI+LiTFSI and assuming that the volume of EMIM-TFSI did not change upon addition of LiTFSI. All calculations are made for 15.0 g MTM57. It should be noted that direct volumetric measurements are complicated by the high viscosity of MTM57.

Table 2. Compositions of epoxy resin based formulations containing EMIM-TFSI, LiTFSI and different amounts of propylene carbonate (PC).

Sample*	EMIM-TFSI +PC+LiTFSI [g]	EMIM-TFSI [g]	LiTFSI [g]	PC [g]
1PC_50MTM57	21.425	10.881	8.765	0.153
5PC_MTM57	21.573	10.507	8.844	0.756
10PC_MTM57	21.768	9.962	9.115	1.51
20PC_MTM57	21.914	8.440	9.509	3.451
50PC_MTM57	22.757	5.569	10.252	7.617
100PC_MTM57	23.319	0	11.309	14.998

*The concentration of LiTFSI in PC + EMIM-TFSI was kept constant at 2.3 mol/l and weight ratio MTM57: (PC+EMIM-TFSI) at 50:50 wt.% All calculations are made for 15.0 g MTM57.

Characterization of structural electrolyte based on epoxy resin

To perform studies on the monolithic samples, discs with a thickness of 2-3 mm were cut from the top and the bottom of the monolith using a dry band saw. Samples for ionic conductivity measurements were polished using 1200 grit sand paper to improve their finish. All samples were dried overnight at 80^{o}C under reduced pressure before testing. For the Raman spectroscopy and ionic conductivity studies, all samples were stored in a glove box in argon atmosphere with less than 1 ppm H_2O and 1 ppm O_2.

Raman spectra were collected at room temperature on a Stand Alone FT-Raman spectrometer (Bruker MultiRAM), using a Nd-YAG laser line at 1064 nm, to minimize detrimental luminescence. The resolution was set to 2 cm^{-1}. The overlapping bands of interest were deconvoluted by fitting Voigt profiles using the PeakFit software. All Raman spectra were analyzed in the range 620-780 cm^{-1} and normalized to the 640 cm^{-1} band (from 625 to 685 cm^{-1}), which is characteristic only for MTM57. The deconvolution analysis concentrated on the TFSI mode due to contraction / expansion of the TFSI^{-} which provides a very strong Raman cross-section[45, 46] within the range 777-720 cm^{-1}; a band representing the "*free"* TFSI anions is found at ~743-737 cm^{-1}, while the band at ~747-751 cm^{-1} corresponds to Li^{+}-coordinated TFSI anions (*e.g.* $[Li(TFSI)_2]^{-}$ species)[47]. Additionally, a minor band at approximately 739 cm^{-1}, originating from MTM57, was included in the deconvolution. To compare the 50MTM57 samples with a reference sample (Li/EMIM-TFSI), all Raman spectra were normalized using the entire TFSI band around 740 cm^{-1}.

The mole fraction of Li cations interacting with the resin was calculated indirectly, from the spectroscopic data for the TFSI bands using the equation below;

"free" Li^+ fraction = ($LiTFSI_{\text{mole fraction}}$ – 0.5 x coordinated $TFSI^-_{\text{mole fraction}}$) / $LiTFSI_{\text{mole fraction}}$

The ionic conductivity of the cured formulations was studied using impedance spectroscopy in two steps. Initially, discs from the top and the bottom of all formulations were tested at room temperature (20-22°C) to check the bulk uniformity of the structural electrolytes. Subsequently, a systematic study of the structural electrolytes over a wide range of temperatures (-30°C to +60°C) was performed by dielectric spectroscopy using a Novocontrol broadband dielectric spectrometer in the frequency range of 10^{-2}-10^7 Hz. Structural electrolytes were placed between two stainless steel electrodes and loaded into a cryo-furnace under nitrogen. Data were collected during heating from -30°C to +60°C in 10°C steps, with a stabilization time of 15 min at each temperature. The DC ionic conductivity data was extracted from the plateau region of each dielectric spectrum.

The glass transition temperature (T_g) of the structural electrolytes was determined using differential thermal-mechanical analysis (DMTA) performed in three-point bending mode over the temperature range from 10 to 300°C and a frequency of 1 Hz. Tests were performed on rectangular samples, width 5.4-6.0 mm, thickness 2-3 mm and span width of 10 mm, cut from the plaques. The T_g values of the structural electrolyte, prior to extraction, were determined from the maximum in the tan δ curves.

Mechanical performance of the cured formulations was characterized using three point bending tests at room temperature. Young's modulus and the bending strength were determined using a Zwick testing frame equipped with a 1 kN load cell and an optical "Heidenhain" displacement transducer. Tests were performed on rectangular samples, length

30-35 mm, width 4 mm, thickness 2-3 mm, cut from the plaques. Young's modulus was calculated from the slope of the initial linear part of the strain/stress response.

To study the morphology and determine the polymer content, EMIM-TFSI and LiTFSI were extracted from the cured formulations as follows. A pre-weighed structural electrolyte, about 0.5 - 1.0 g, was placed in a glass vial filled with ethanol, which was changed twice a day, for at least one week, and subsequently dried in an oven at 70°C under reduced pressure to constant weight. The amount of electrolyte extracted from the sample was estimated from the change in mass.

SEM (Jeol JSM 5610 LV) micrographs of samples after electrolyte extraction were recorded at an acceleration voltage of 15 kV. Cryofractured samples were mounted on the stub using a carbon adhesive and gold coated for 120 s in an argon atmosphere (Emitech 550). To estimate the extent to which the microstructure became finer and more uniform, the size of the nodules was determined using the software ImageJ, measuring at least 100 spherical nodules per sample.[26]

RESULTS AND DISCUSSION

Two main approaches were explored with the aim of producing structural electrolytes with bicontinuous structures; changing the epoxy curing rate by varying the curing temperature and increasing the solubility of the resin in the electrolyte.

Effect of curing temperature on the morphology

Varying the curing temperature from 80°C to 140°C did not lead to the desired microstructures, but did influence the stability of the blends; for example, formulations cured at 100°C and above resulted in macroscopically homogeneous samples, while formulations cured at 80°C formed macroscopically heterogeneous (grossly phase separated) samples, consisting of two clearly macroscopically separated phases, a polymer-rich upper and an

electrolyte-rich lower layer (further details of the curing procedure can be found in the Supporting Information, including SEM micrographs of samples cured at 100°C and 140°C, Figure SI 1). Whilst higher curing temperatures favor miscibility of the components, an effective bicontinuous structure relies on phase segregation of a miscible mixture during the curing process.[10] The blend must initially form a stable emulsion or preferably a fully miscible molecular mixture at temperatures lower than the curing temperature which is subsequently destabilized, i.e. phase separates, during curing. Depending on the miscibility of MTM57 with electrolyte, two different types of microstructures were formed, as schematically shown in Figure. **1**. In the case of full miscibility of the components (Figure. **1**a), pre-cure, a simple bicontinuous structure formed, whereas partial miscibility (Figure. **1**b) led to the formation of more complex multiscale microstructures.

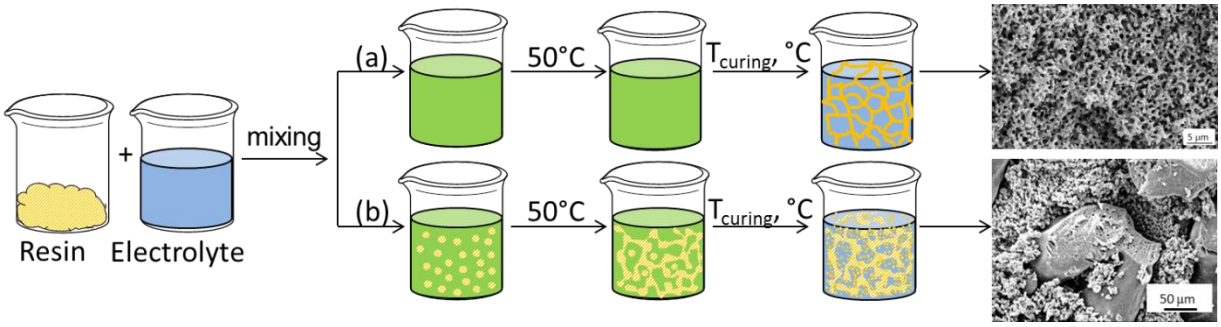

Figure. 1. Schematic of the formation of different types of microstructures from (a) fully miscible and (b) partially miscible formulations.

Effect of the LiTFSI concentration on the morphology and properties

The addition of a lithium salt to an IL most often leads to a decrease in the total ionic conductivity because of the associated increase in viscosity and a reduction of the mobility of the carrier ions.[48-50] Nevertheless, here, the presence of LiTFSI is essential, as it allows the formation of macroscopically homogeneous samples. In the absence of LiTFSI, macroscopically homogeneous samples were only obtained at high epoxy resin contents (>70

wt.% (70MTM57)); however, high resin content resulted in samples with microstructures (Figure 2) consisting of IL droplets dispersed in the bulk epoxy phase. This closed pore morphology resulted in materials with a high Young's modulus of 2.29 ± 0.23 GPa and flexural strength of 115.5 ± 0.4 MPa, comparable to the neat MTM57 (Young's modulus 2.73 GPa and flexural strength 145.3 MPa), but negligible ionic conductivity of around $6x10^{-8}$ mS/cm.

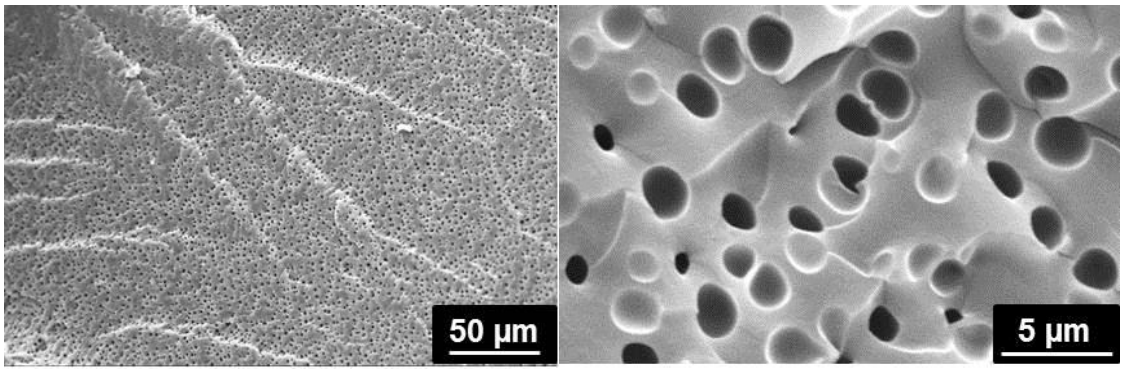

Figure 2. SEM micrographs at different magnifications of structural electrolytes with MTM57:EMIM-TFSI ratio 70:30 wt.% (70MTM57) without LiTFSI, after EMIM-TFSI extraction.

The importance of LiTFSI as a stabilizing or solubilizing component of the structural electrolyte correlates with literature showing that, for example, the presence of LiTFSI in ILs improved cellulose solubility.[49] To identify the optimum LiTFSI concentration for the current system, the concentration of LiTFSI in EMIM-TFSI was varied from 0.5mol/l to 4.6 mol/l with the maximum concentration determined by the LiTFSI solubility limit. Increasing LiTFSI concentration was expected to improve the solubility of MTM57 in the electrolyte,[49] delaying the phase separation process occurring during curing, in turn leading to the formation of a finer bicontinuous pore structure. By monitoring the polymer content (Figure 3) and ionic conductivity (Figure SI 2) of the top and bottom parts of the cylindrical structural electrolytes, it was clear that the LiTFSI concentration should be at least 2.3 mol/l to obtain a

macroscopically homogeneous cured material from 50:50 mixture of resin:IL (Figure 3, Figure SI 2). In addition, it was observed that an increase in the LiTFSI concentration led to an increase in the transparency of the MTM57+EMIM-TFSI+LiTFSI mixture prior to curing. The formulation containing 2.3 mol/l LiTFSI was a white viscous emulsion even at 70°C, while the formulation containing 4.6 mol/l LiTFSI was an amber colored viscous and visually transparent liquid even at 30°C. The increase in transparency suggests an increasing molecular miscibility which can be attributed to increased interactions between the components of the formulations; for example, Li^+ can coordinate to the epoxy component. Specifically, when mixing LiTFSI with EMIM-TFSI, Li cations complex with TFSI anions of EMIM-TFSI to form $[Li(TFSI)_2]^-$,[47] leaving the EMIM cations "free" to interact with amines[51] and epoxies. Spectroscopic results presented below support these suggestions.

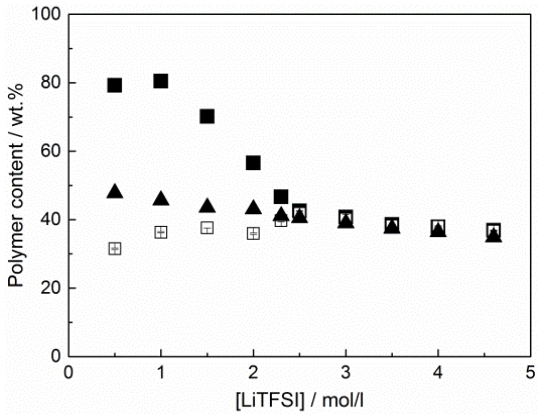

Figure 3. Effect of LiTFSI concentration on the polymer content for 50MTM57 based structural electrolytes: ■ top part; □ bottom part of the sample; ▲ theoretical value.

The morphology of the structural electrolytes also showed a significant dependence on the LiTFSI concentration; for the macroscopically heterogeneous sample (grossly phase separated) containing 0.5 mol/l LiTFSI, there is a clear difference in morphology between the top and bottom parts in a single sample as shown in Figure 4. The top part consists of discrete spherical domains of the IL based electrolyte randomly dispersed in the continuous epoxy

matrix (Figure 4a), whilst the bottom part comprises a network of connected spherical epoxy nodules (Figure 4b).

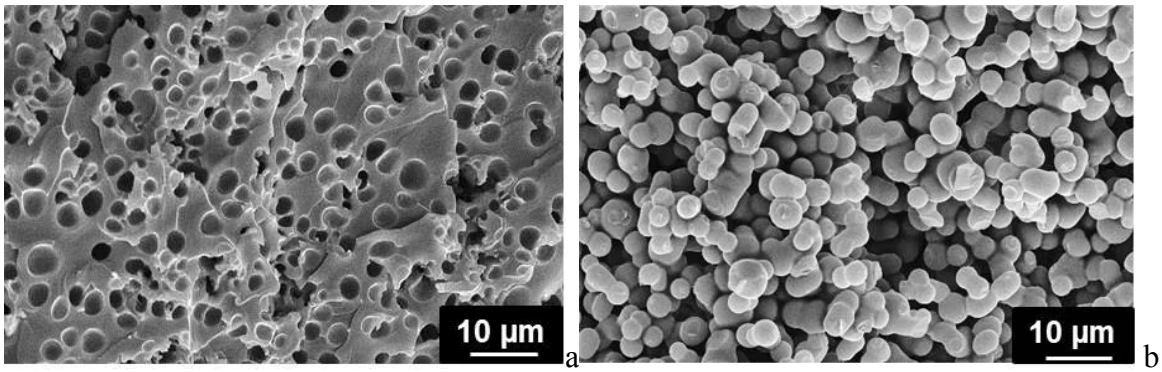

a b

Figure 4. SEM micrographs of 50MTM57 containing 0.5 mol/l LiTFSI in IL based electrolyte (0.5M_50MTM57): a – top part; b – bottom part of the sample. Images were taken after extraction of the EMIM-TFSI+LiTFSI electrolyte.

Samples with LiTFSI concentrations of 2.3 mol/l or higher all have a combination of two morphologies. A continuous epoxy phase (coarse phase), the cross section (100±60 µm) of which exhibit discrete spherical pores with an average pore size of 1.6±0.5 µm similar to those observed in the top part of the 0.5M_50MTM57 sample (Figure 4a), is surrounded by a network of connected spherical nodules with diameter 3.4±0.6 µm. Further increases in the LiTFSI concentration caused the structural features of both phases to become finer and more uniform (Figure 5, Figure SI 4). A reduction in the length scale of the microstructural features was anticipated since increasing LiTFSI concentration increased miscibility of the components and, therefore, reduced the driving force for phase segregation in the window available for curing.

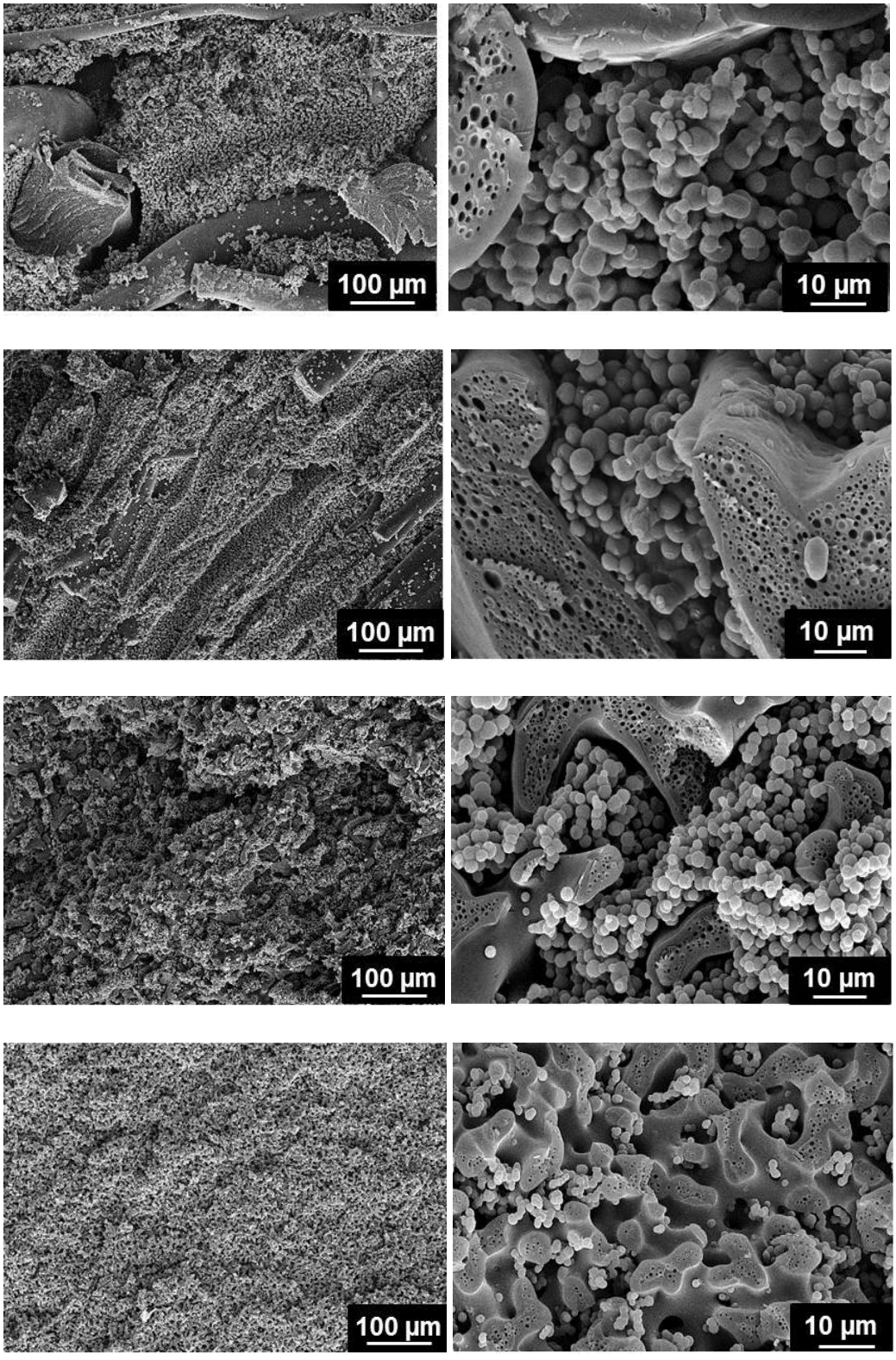

Figure 5. SEM micrographs of 50MTM57 structural electrolytes containing IL based electrolytes with different LiTFSI concentrations: a - 2.3 mol/l; b – 3.0 mol/l; c - 4.0 mol/l; d

– 4.6 mol/l. Two different magnifications are presented for each sample and all images were obtained after extraction of the EMIM-TFSI+LiTFSI electrolyte.

Since the ionic conductivity depends on the type and concentration of charge carriers, the nature of the LiTFSI interaction with the bulk TFSI anions is of interest. Raman spectroscopy analysis shows that the number of "free" TFSI anions in the structural 50MTM57 electrolytes decreased with increasing LiTFSI concentration, most likely due to the formation of $[Li(TFSI)_2]^-$ complexes (Figure 6).[47] The molar fraction of Li cations interacting with the resin (Figure 7) was indirectly determined using the spectroscopic data (Table 3). The percentage of "free" TFSI anions for the structural electrolytes was 2-6 times higher than for the reference sample (EMIM-TFSI+LiTFSI). This striking difference suggests that the Li cations prefer to interact with functional groups of the epoxy resin rather than forming $[Li(TFSI)_2]^-$ complexes. The data indicate that dynamic cross-links are formed between the epoxy and the Li cations [52, 53] due to electrostatic interactions resulting in temporary connections, which may further influence the resulting morphologies (Figure 5) and are consistent with the suggestion that most of the ionic conductivity is carried by the TFSI and EMIM ions, rather than by the Li cations. The maximum interaction between the Li cations and the epoxy is observed at 3.5 mol/l LiTFSI (Figure 7); thereafter, the formation of $[Li(TFSI)_2]^-$ complexes starts to dominate leading to a dramatic drop in the ionic conductivity and an increase in mechanical performance as discussed below (Figure 11). The increase in $[Li(TFSI)_2]^-$ complex formation also led to an increasing concentration of "free" EMIM cations relative to all other species, promoting additional reactions with epoxy resin, as it is known[31] that imidazole and its derivatives can act as a catalyst for the epoxy ring opening polymerization.[20]

Table 3 Results of the deconvolution analysis of the Raman spectra.

[LiTFSI] [mol/l]	LiTFSI mole fraction	Amount of TFSI top part (t)		Amount of TFSI bottom part (b)		Reference sample		b/t 740 cm^{-1} band ratio
		"Free"	Li^+ coord.	"Free"	Li^+ coord.	"Free"	Li^+ coord.	
2.3	0.37	79%	21%	80%	20%	38%	62%	1.40
3.0	0.43	74%	26%	73%	27%	-	-	1.09
3.5	0.47	67%	33%	66%	34%	30%	70%	1.04
4.0	0.50	63%	37%	63%	37%	-	-	1.01
4.6	0.55	51%	49%	51%	49%	9%	91%*	1.02

* - LiTFSI crystallized out of solution during the measurement.

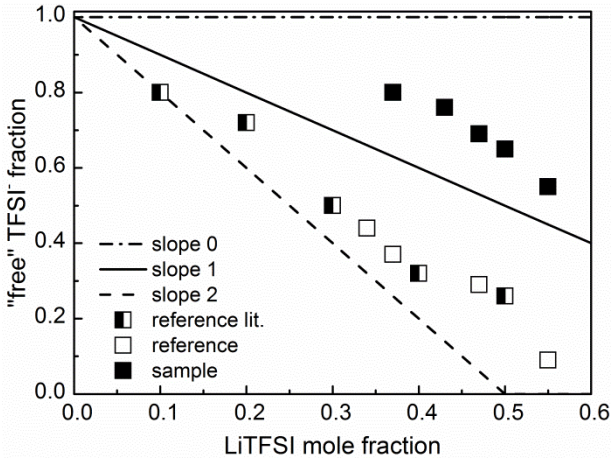

Figure 6. The mole fraction of Li^+ interacting with the resin as a function of the LiTFSI mole fraction. Literature data were extracted from ref. 47. Slope 0 (y=1): represents a theoretical situation in which Li^+ does not interact with TFSI; slope 1**:** represents a theoretical situation in which each Li^+ interacts only with one TFSI anion; slope 2: represents a theoretical situation in which each Li^+ interacts with two TFSI anions.

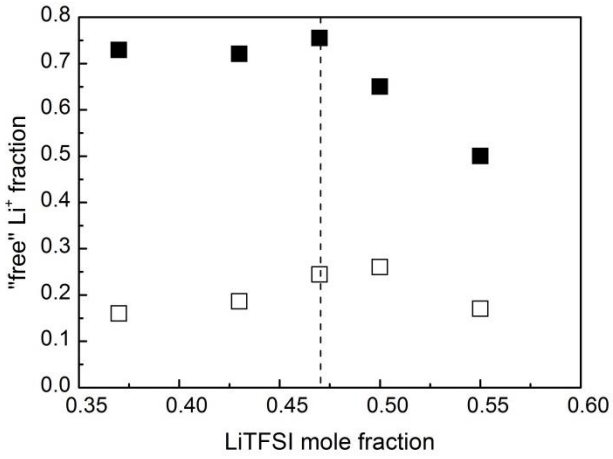

Figure 7. Plot of "free" Li^+ fraction as a function of LiTFSI mole fraction. (■– sample, □ – reference (EMIM-TFSI+LiTFSI only)).

In order to characterize the ion conductivity of the prepared structural electrolytes, temperature dependent measurements were carried out using dielectric spectroscopy (Figure 8). The ionic conductivity increases with increasing temperature in a non-linear fashion, following the traditional polymer electrolyte VTF behavior and thus suggesting that the ion transport is coupled to the relaxation dynamics of the matrix. The decrease in ionic conductivity with increasing LiTFSI concentration was expected due to the increase in viscosity of the electrolyte, reduction of the mobility of the carrier ions, the increased aggregation of charge carriers,[48, 50, 54] as well as the reduced microstructural length scale, which all may alter the transport properties. Although the microstructure must also contribute, the increase in storage modulus determined from the DMTA experiments (0.31 GPa at 2.3 mol/l LiTSFI to 0.89 GPa at 4.6 mol/l) could indicate an increased crosslink density and reduced chain mobility. The average molecular weight between crosslinks (M_c) was calculated (Table SI1) using simple rubber elasticity theory, which is widely used for epoxy based systems.[55, 56] It is to be expected that the sample with the likely highest crosslinking density and lowest chain mobility, 4.6 mol/l LiTFSI, will have the lowest ionic conductivity, as indeed observed.

Three point bending tests (Figure 9) also confirmed that increasing the LiTFSI content led to increased stiffness, elongation at break, and strength. The improvements are mainly manifested between 3.0 and 4.0 mol/l LiTFSI (Figure 10). The increase of the mechanical performance with the LiTFSI concentration can be explained by a combination of two factors. One is the increase in effective crosslinking density / reduction of M_c , as discussed above. Another factor is the change in the microstructure (Figure 5, Figure SI 3), more specifically the reduction of the continuous (coarse) epoxy phase dimensions and increase of their number per area as determined from the SEM micrographs.

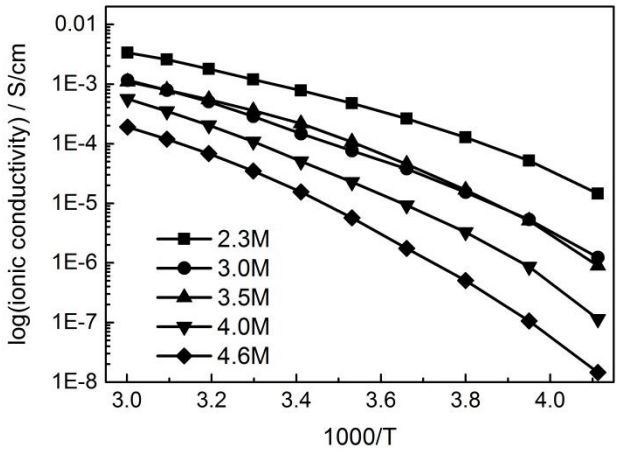

Figure 8. Temperature dependence of ionic conductivity for 50MTM57 structural electrolytes containing IL based electrolytes with different LiTFSI concentrations. As these samples are all macroscopically homogeneous, only results for the bottom of the samples are shown.

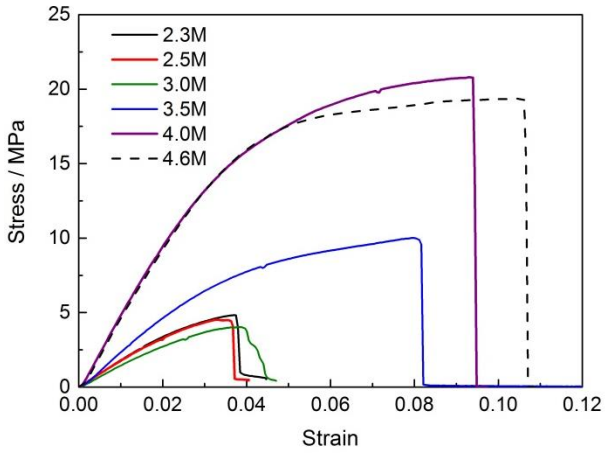

Figure 9. Typical stress-strain curves as a function of the LiTFSI concentration for 50MTM57 structural electrolytes.

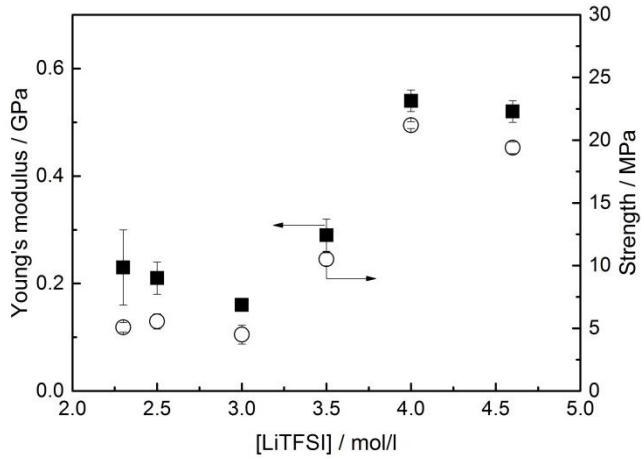

Figure 10. Effect of LiTFSI concentration on Young's modulus and strength for structural 50MTM57 electrolytes.

The relationship between the Young's modulus and the room temperature ionic conductivity of these 50MTM57 structural electrolytes with different concentrations of LiTFSI show a typical inversely-related trend such that an increase in the mechanical performance leads to a drop in the ionic conductivity (Figure 11). However, the effect of the LiTFSI concentration was more pronounced on ionic conductivity, for which values varied in two orders of magnitude range, compared to mechanical properties, for which all values were of the same order of magnitude.

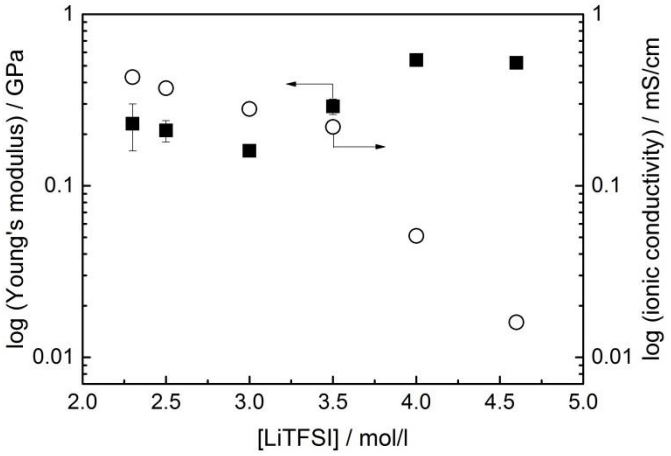

Figure 11. Ionic conductivity and Young's modulus as functions of LiTFSI concentration in the 50MTM57 structural electrolytes.

Effect of organic solvent addition on the morphology and properties

The MTM57 resin must be miscible with the IL based electrolyte in order to generate a favorable morphology, which requires use of LiTFSI, but at the same time this addition tends to reduce the ionic conductivity through the formation of $[Li(TFSI)_2]^-$ complexes; for this reason, other routes to compatibilization are of interest. One possibility is the addition of an organic solvent with a high dielectric constant,[57] and good electrochemical stability, such as propylene carbonate (PC). Substituting 5 wt.% or more of EMIM-TFSI with an equal amount of PC changed the appearance of the uncured mixtures, from white highly viscous pastes to amber-colored transparent viscous liquids. After curing, the monoliths with 1 wt.% PC were white solids, indicating macro-phase separation, while samples containing only LiTFSI in PC (no EMIM-TFSI) as the electrolyte were amber-colored nearly transparent rubber like materials (Figure SI 4). The observed formation of a rubbery gel-like material suggests that the solubility of MTM57 in the electrolyte increased with PC content, not only prior to curing but also in the early stages of the curing process, preventing phase separation. The morphology of the structural electrolyte prepared with 1 wt.% PC added to the formulation

containing 2.3 mol/l LiTFSI (1PC_50MTM57) (Figure 12) resembles that of the structural electrolyte with 4.6 mol/l LiTFSI (4.6M_50MTM57) (Figure 5; Figure 12a). In other words, PC seems to play a similar role to that of a high concentration of LiTFSI. The gelled samples containing more than 5 wt.% PC do not possess any permanent porosity, as detectable by SEM after extraction of the electrolyte (Figure 12b).

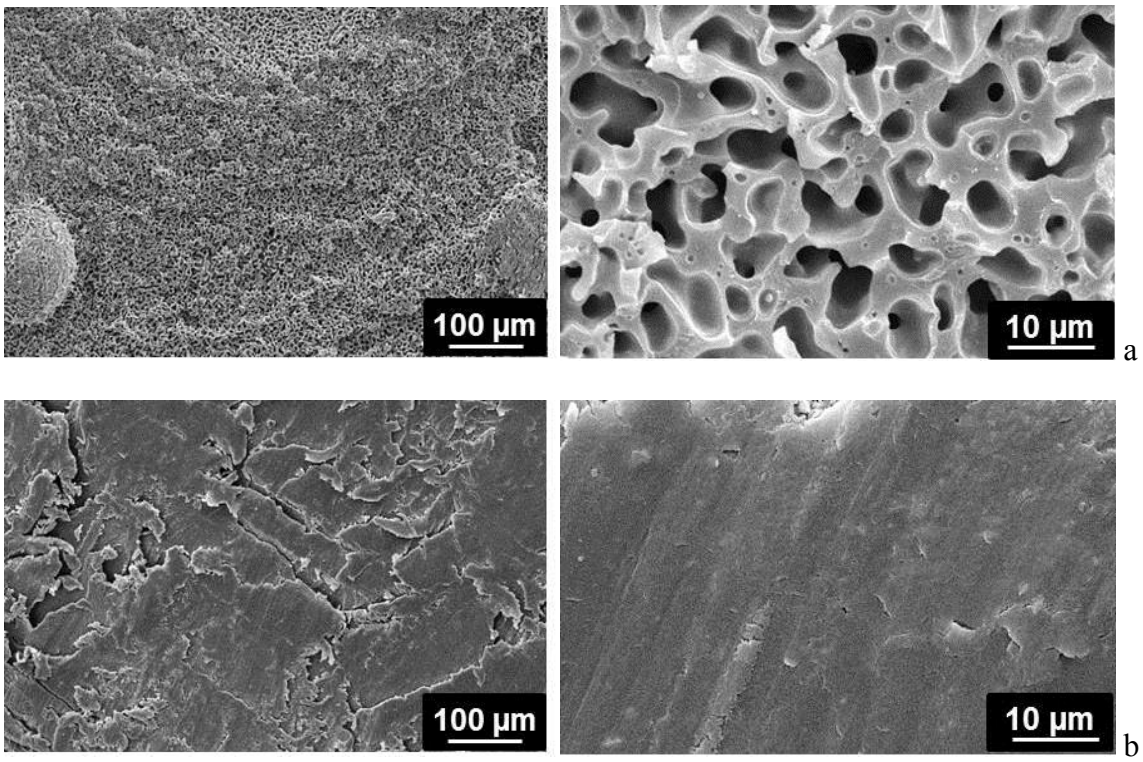

Figure 12. SEM micrographs of structural electrolytes with 2.3 mol/l LiTFSI (2.3M_50MTM57) containing 1 wt.% (a) and 5 wt.% (b) PC. Two magnifications are presented for each sample; all images were taken after extraction of the EMIM-TFSI+LiTFSI electrolyte.

The similar ionic conductivity of the top and the bottom parts of the monoliths showed that all samples were macroscopically homogeneous (Figure SI 5). Temperature dependent measurements showed that the VTF behavior is retained, with decreased curvature and increased slope for the 5 wt.% PC electrolyte (Figure 13). Substitution of 1 wt.% EMIM-

TFSI by 1 wt.% PC led to a decrease of the room temperature ionic conductivity for the resulting structural electrolyte; from 0.43 mS/cm to 0.15 mS/cm. This outcome was somewhat unexpected, as previous literature suggests that PC can interact with Li^+ reducing formation of $[Li(TFSI)_2]^-$ complexes.[57, 58] Since the $[Li(TFSI)_2]^-$ complexes are responsible for the increase in viscosity and the decrease in ionic conductivity of LiTFSI-doped IL, a reduction of their number might be expected to improve ionic conductivity. For the structural electrolyte containing 1 wt.% PC, the proportion of "free" TFSI anions was 89%, which is slightly higher than for the analogous sample without any PC (2.3M_50MTM57 approx. 80%). This change suggests that PC indeed coordinate Li cations leading to a reduction of $[Li(TFSI)_2]^-$ complexes formation, thereby releasing two TFSI anions per PC-coordinated Li^+. The decrease in ionic conductivity observed may be due to various factors, including swelling of the epoxy chains by the electrolyte, potential reactions of the cyclic carbonate with the primary amine of the formulation leading to the formation of hydroxyl-urethane groups[59], or the decreased microstructural length scale. PC also had a plasticizing effect as the T_g decrease from 111°C for 2.3M_50MTM57 to 65°C upon addition of 1 wt.% PC.

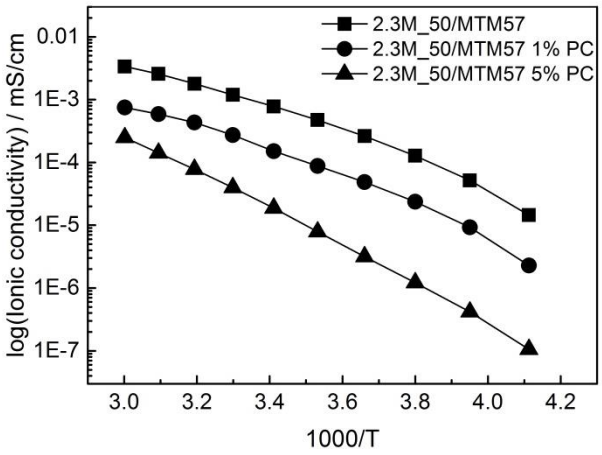

Figure 13. Temperature dependence of the ionic conductivity of structural electrolytes based on 2.3M_50MTM57 containing different amounts of PC.

However, if structural electrolytes with similar characteristic microstructural length scales (with diameter of the coarse epoxy phase around 2-4 μm), are compared, i.e. 4.6M_MTM57 with 1PC_50MTM57, the latter has a higher ionic conductivity. This improvement can be attributed to a combination of a reduced viscosity and the changes in the charge carrier species. The addition of 5 wt.% of PC resulted in a sample with an order of magnitude lower ionic conductivity, in this case due to the absence of any permanent porosity (Figure 12).

Replacing only 1 wt.% IL with PC also led to a significant improvement in the overall mechanical performance. The Young's modulus increased from 0.23 ± 0.07GPa to 0.90 ± 0.03 GPa which may be caused by the decrease of the size scale of the coarse continuous epoxy phase from ~100 μm to ~2 μm (Figure 4 and Figure **12**), since the average molecular weight between crosslinks (M_c) value decreased only slightly from 4576 g/mol to 4489 g/mol and T_g is significantly lower with PC (65°C compared to 2.3M_50MTM57 111°C). The Young's modulus for 4.6M_50MTM57 (0.52 GPa) fits this trend, with an intermediate value between those for structural electrolytes 2.3M_50MTM57 with and without PC.

CONCLUSIONS

The morphology of structural electrolytes, based on a fully-formulated, commercially-available epoxy resin MTM57 and IL based electrolyte, depends on the miscibility of the components prior to and during curing, which in turn depends on the composition and curing temperature. The effect of the morphology on the properties of the resulting structural electrolytes was studied in detail. The composition played a more significant role in determining the morphology than the curing temperature. Samples cured below 100°C underwent a dramatic phase separation resulting in macroscopically heterogeneous materials. An increase in the LiTFSI concentration in the IL based electrolyte (EMIM-TFSI+LiTFSI) led to the formation of stabilized, macroscopically homogeneous materials and gradually

finer microstructures. Increased mechanical properties and an associated reduction in ionic conductivities were explained by a combination of factors including changes in morphology, increases in (dynamic) cross-linking density, and altered Li^+-TFSI interactions. The addition of PC, an organic solvent with high dielectric constant, resulted in an increased solubility of MTM57 in the IL electrolyte and, after curing, resulted in structural electrolytes with a wide range of physical properties, from white solids to amber-colored rubber-like materials. Changes in the microstructure, including a decreased characteristic length scale, led to a four-fold improvement in the Young's modulus accompanied by a three-fold reduction in the ionic conductivity. These structural electrolytes show ionic conductivities suitable for applications in structural energy storage devices across a wide temperature range. The addition of aprotic solvents and different salts might allow for further optimization of the morphology and properties. In general, a homogeneous bicontinuous network of two pure and distinct phases is desirable, one for mechanical performance and one for ionic transport, at a characteristic length scale defined by the other features within the device (for example, the diameter of reinforcing fibre electrodes). To achieve this bicontinuous structure, an initially miscible system must switch to very low miscibility during curing, leading to phase separation into the desired structure. Additional hierarchical features created by a more complex phase behavior may be advantageous, particularly for maximizing the ion transport[10] and different property envelopes will indeed be needed for structural batteries and supercapacitors, respectively, or indeed potential application as robust electrolytes for more conventional electrochemical devices.

Acknowledgements: Funding from the EU as part of the FP7 project "Storage" (Grant Agreement No.234236) is gratefully acknowledged. Authors would like to acknowledge

Cytec Industries for providing the resin for the study and Mr J. Cole for the help with sample preparation.

Dedications

The authors commemorate the late colleagues Dr. Joachim H. G. Steinke (1964−2013) and Prof. Per Jacobsson (1958-2013) for their contributions to this work.

ASSOCIATED CONTENT

Supporting information

(1) Details on effect of the curing temperature on the morphology of the epoxy based formulations, including SEM micrographs; (2) Figures showing an effect of LiTFSI and PC content on ionic conductivity; (3) Images showing the appearance of the structural electrolytes depending on PC content; (4) Table showing the effect of LiTFSI concentration on thermo mechanical properties. This material is available free of charge via the Internet at http://pubs.acs.org.

AUTHOR INFORMATION

Corresponding Authors

* (NSh) email: n.shirshova@imperial.ac.uk; phone: +44(0)2075940855
* (PJ) email: patrik.johansson@chalmers.se; phone: +46 (0)31 772 31 78

Author Contributions

The manuscript was written through contributions of all authors. All authors have given approval to the final version of the manuscript.

Funding Sources

Funding from the EU as part of the FP7 project "Storage" (Grant Agreement No.234236) is gratefully acknowledged.

REFERENCES

(1) Ahmad, S. Polymer Electrolytes: Characteristics and Peculiarities. *Ionics* **2009**, *15*, 309-321.
(2) Quartarone, E.; Mustarelli, P. Electrolytes for Solid-State Lithium Rechargeable Batteries: Recent Advances and Perspectives. *Chem. Soc. Rev.* **2011**, *40*, 2525-2540.
(3) Scrosati, B.; Garche, J. Lithium Batteries: Status, Prospects and Future. *J. Power Sources* **2010**, *195*, 2419-2430.
(4) Mukherjee, R.; Krishnan, R.; Lu, T.-M.; Koratkar, N. Nanostructured Electrodes for High-Power Lithium Ion Batteries. *Nano Energy* **2012**, *1*, 518-533.
(5) Zhang, L. C.; Sun, X.; Hu, Z.; Yuan, C. C.; Chen, C. H. Rice Paper as a Separator Membrane in Lithium-Ion Batteries. *J. Power Sources* **2012**, *204*, 149-154.
(6) Snyder, J. F.; Wetzel, E. D.; Watson, C. M. Improving Multifunctional Behavior in Structural Electrolytes through Copolymerization of Structure- and Conductivity-Promoting Monomers. *Polymer* **2009**, *50*, 4906-4916.
(7) Kovačič, S.; Kren, H.; Krajnc, P.; Koller, S.; Slugovc, C. The Use of an Emulsion Templated Microcellular Poly(Dicyclopentadiene- Co - Norbornene) Membrane as a Separator in Lithium-Ion Batteries. *Macromol. Rapid Commun.* **2013**, *34*, 581−587.
(8) Qian, H.; A.R. Kucernak; E.S. Greenhalgh; A. Bismarck; Shaffer, M. S. P. Multifunctional Structural Supercapacitor Composites Based on Carbon Aerogel Modified High Performance Carbon Fiber Fabric. *ACS Appl. Mater. Interfaces* **2013**, *5* 6113-6122.
(9) Shirshova, N.; Johansson, P.; Marczewski, M. J.; Kot, E.; Ensling, D.; Bismarck, A.; Steinke, J. H. G. Polymerised High Internal Phase Ionic Liquid-in-Oil Emulsions as Potential Separator for Lithium Ion Batteries. *J. Mater. Chem.* **2013**, *1*, 9612-9619.
(10) Shirshova, N.; Bismarck, A.; Carreyette, S.; Fontana, Q. P. V.; Greenhalgh, E. S.; Jacobsson, P.; Johansson, P.; Marczewski, M. J.; Scheers, J.; Kalinka, G., et al. Structural Supercapacitor Electrolytes Based on Bicontinuous Ionic Liquid–Epoxy Resin Systems. *J. Mater. Chem. A* **2013** *1*, 15300–15309.
(11) Snyder, J. F.; Carter, R. H.; Wetzel, E. D. Electrochemical and Mechanical Behavior in Mechanically Robust Solid Polymer Electrolytes for Use in Multifunctional Structural Batteries. *Chem. Mater.* **2007**, *19*, 3793-3801.
(12) Pereira, T.; Guo, Z.; Nieh, S.; Arias, J.; Hahn, H. T. Energy Storage Structural Composites: A Review. *J. Comp. Mater.* **2009**, *43*, 549-560.
(13) Ichino, T.; Matsumoto, M.; Takeshita, Y.; Rust, J. S.; Nishi, S. New Concept for Polymer Electrolyte: Dual-Phase Polymer Electrolyte. *Electrochim. Acta* **1995**, *40*, 2265-2268.
(14) Matsumoto, M. Polymer Electrolytes with a Dual-Phase Structure Composed of Poly(Acrylonitrileco-Butadiene)Lpoly(Styrene-Co-Butadiene) Blend Films Impregnated with Lithium Salt Solution. *Polymer* **1996**, *37*, 625-631.

(15) Gayet, F.; L.Viau; Leroux, F.; Mabille, F.; Monge, S.; Robin, J. J.; Vioux, A. Unique Combination of Mechanical Strength, Thermal Stability, and High Ion Conduction in PMMA-Silica Nanocomposites Containing High Loadings of Ionic Liquid. *Chem. Mater.* **2009**, *21*, 5575-5577.
(16) Ji, J.; Li, B.; Zhong, W.-H. Simultaneously Enhancing Ionic Conductivity and Mechanical Properties of Solid Polymer Electrolytes Via a Copolymer Multi-Functional Filler. *Electrochim. Acta* **2010**, *55*, 9075-9082.
(17) Krebs, H.; Yang, L.; Shirshova, N.; Steinke, J. H. G. A New Series of Cross-Linked (Meth)Acrylate Polymer Electrolytes for Energy Storage. *React. Funct. Polym.* **2012**, *72*, 931-938.
(18) Matsumoto, K.; Endo, T. Confinement of Ionic Liquid by Networked Polymers Based on Multifunctional Epoxy Resins. *Macromolecules* **2008**, *41*, 6981-6986.
(19) K. Matsumoto; Endo, T. Synthesis of Networked Polymers by Copolymerization of Monoepoxy-Substituted Lithium Sulfonylimide and Diepoxy-Substituted Poly(Ethylene Glycol), and Their Properties. *J. Polym. Sci. Part A: Polym. Chem.* **2011**, *49*, 1874-1880.
(20) Tsujioka, N.; Ishizuka, N.; Tanaka, N.; Kubo, T.; Hosoya, K. Well-Controlled 3D Skeletal Epoxy-Based Monoliths Obtained by Polymerization Induced Phase Separation. *J. Polym. Sci. Part A: Polym. Chem.* **2008**, *46*, 3272-3281.
(21) Shen, Y.; Qi, L.; Mao, L. Macroporous Polymer Monoliths with a Well-Defined Three Dimensional Skeletal Morphology Derived from a Novel Phase Separator for Hplc. *Polymer* **2012**, *53*, 4128-4134.
(22) Luo, Y.-S.; Cheng, K.-C.; Wu, C.-L.; Wang, C.-Y.; Tsai, T.-H.; Wang, D.-M. Preparation of Epoxy Monoliths Via Chemically Induced Phase Separation. *Colloid. Polym. Sci.* **2013**, *291*, 1903–1912.
(23) Kanamori, K.; Nakanishi, K.; Hanada, T. Rigid Macroporous Poly(Divinylbenzene) Monoliths with a Well-Defined Bicontinuous Morphology Prepared by Living Radical Polymerization. *Adv. Mater.* **2006**, *18*, 2407-2411.
(24) Nguyen, A. M.; Irgum, K. Epoxy-Based Monoliths. A Novel Hydrophilic Separation Material for Liquid Chromatography of Biomolecules. *Chem. Mater.* **2006**, *18*, 6308-6315.
(25) Rico, M.; López, J.; Montero, B.; Bellas, R. Phase Separation and Morphology Development in a Thermoplastic-Modified Toughened Epoxy. *Eur. Polym. J.* **2012**, *48*, 1660-1673.
(26) López, J.; Rico, M.; Ramírez, C.; Montero, B. Epoxy Resin Modified with a Thermoplastic. Influence of Modifier and Reaction Temperature on the Phase Separation. *J. Therm. Anal. Calorim.* **2010**, *99*, 75-81.
(27) Oyanguren, P. A.; Galante, M. J.; Andromaque, K.; Frontini, P. M.; Williams, R. J. J. Development of Bicontinuous Morphologies in Polysulfone–Epoxy Blends. *Polymer* **1999**, *40*, 5249-5255.
(28) Ratna, D. Phase Separation in Liquid Rubber Modified Epoxy Mixture. Relationship between Curing Conditions, Morphology and Ultimate Behavior. *Polymer* **2001**, *42*, 4209-4218.
(29) Soulé, E.; Mata, M. G. d. l.; Borrajo, J.; Oyanguren, P. A.; Galante, M. J. Reaction-Induced Phase Separation in an Epoxy/Low Molecular Weight Solvent System. *J. Mater. Sci.* **2003**, *38*, 2809 - 2814.
(30) Zhang, R.; Zhang, L. Preparation of 3-Dimentional Skeletal Polymer Via Control of Reaction-Induced Phase Separation in Epoxy/Poly(Ethylene Glycol) Blends. *Polymer Bulletin* **2008**, *61*, 671-677.
(31) Maka, H.; Spychaj, T.; Pilawka, R. Epoxy Resin/Ionic Liquid Systems: The Influence of Imidazolium Cation Size and Anion Type on Reactivity and Thermomechanical Properties. *Ind. Eng. Chem. Res.* **2012**, *51*, 5197−5206.

(32) Sanes, J.; Carrión-Vilches, F. J.; Bermúdez, M. D. New Epoxy-Ionic Liquid Dispersions. Room Temperature Ionic Liquid as Lubricant of Epoxy Resin-Stainless Steel Contacts *e-Polymers* **2007**, *005*, 1-12.
(33) Soares, B. G.; Livi, S.; Duchet-Rumeau, J.; Gerard, J.-F. Synthesis and Characterization of Epoxy/Mcdea Networks Modified with Imidazolium-Based Ionic Liquids. *Macromol. Mater. Eng.* **2011**, *296*, 826-834.
(34) Baker, G. A.; Baker, S. N.; Pandey, S.; Bright, F. V. An Analytical View of Ionic Liquids. *Analyst* **2005**, *130*, 800-808.
(35) Sato, T.; Masuda, G.; Takagi, K. Electrochemical Properties of Novel Ionic Liquids for Electric Double Layer Capacitor Applications. *Electrochim. Acta* **2004**, *49*, 3603-3611.
(36) M. Galiński; A. Lewandowski; Stępniak, I. Ionic Liquids as Electrolytes. *Electrochim. Acta* **2006**, *51*, 5567-5580.
(37) Paulechka, Y. U.; Kabo, A. G.; Blokhin, A. V.; Kabo, G. J.; Shevelyova, M. P. Heat Capacity of Ionic Liquids: Experimental Determination and Correlations with Molar Volume. *J. Chem. Eng. Data* **2010**, *55*, 2719-2724.
(38) A. Lewandowski; Świderska-Mocek, A. Ionic Liquids as Electrolytes for Li-Ion Batteries—an Overview of Electrochemical Studies. *J. Power Sources* **2009**, 601-609.
(39) Kubisa, P. Ionic Liquids as Solvents for Polymerization Processes—Progress and Challenges. *Prog. Polym. Sci.* **2009**, *34*, 1333-1347.
(40) Torimoto, T.; Tsuda, T.; Okazaki, K. i.; Kuwabata, S. New Frontiers in Materials Science Opened by Ionic Liquids. *Adv. Mater.* **2010**, *22*, 1196-1221.
(41) Rahmathullah, M. A. M.; Jeyarajasingam, A.; Merritt, B.; M.VanLandingham; McKnight, S. H.; Palmese, G. R. Room Temperature Ionic Liquids as Thermally Latent Initiators for Polymerization of Epoxy Resins. Communications to the Editor. *Macromolecules* **2009**, *42*, 3219-3221.
(42) Maka, H.; Spychaj, T. Epoxy Resin Crosslinked with Conventional and Deep Eutectic Ionic Liquids. *Polimery* **2012**, *57*, 456-462.
(43) Ostrowska, S.; Markiewicz, B.; Wąsikowska, K.; Bączek, N.; Pernak, J.; Strzelec, K. Epoxy Resins Cured with Ionic Liquids as Novel Supports for Metal Complex Catalysts. *C. R. Chimie* **2013**, *16*, 752-760.
(44) Silva, A. A.; Livi, S.; Netto, D. B.; Soares, B. G.; Duchet, J.; Gérard, J.-F. New Epoxy Systems Based on Ionic Liquid. *Polymer* **2013**, *54*, 2123-2129.
(45) Rey, I.; Johansson, P.; Lindgren, J.; Lassègues, J. C.; J. Grondin; Servant, L. Spectroscopic and Theoretical Study of $[(CF_3SO_2)_2N^-$(TFSI$^-$) and (CF_3SO_2)NH (HTFSI). *J. Phys. Chem. A.* **1998**, *102*, 3249-3258.
(46) Herstedt, M.; Smirnov, M.; Johansson, P.; Chami, M.; Grondin, J.; Servant, L.; Lassègues, J. C. Spectroscopic Characterization of the Conformational States of the Bis(Trifluoromethanesulfonyl)Imide Anion (TFSI$^-$). *J. Raman Spectrosc.* **2005**, *36*, 762-770.
(47) Lassègues, J. C.; Grondin, J.; Aupetit, C.; Johansson, P. Spectroscopic Identification of the Lithium Ion Transporting Species in LiTFSI-Doped Ionic Liquids. *J. Phys. Chem. A* **2009**, *113*, 305-314.
(48) Seki, S.; Kobayashi, Y.; Miyashiro, H.; Ohno, Y.; Usami, A.; Mita, Y.; Kihira, N.; Watanabe, M.; N.Terada Lithium Secondary Batteries Using Modified-Imidazolium Room-Temperature Ionic Liquid. *J. Phys. Chem. B Letters* **2006**, *110*, 10228-10230.
(49) Xu, A.; Wang, J.; Wang, H. Effects of Anionic Structure and Lithium Salts Addition on the Dissolution of Cellulose in 1-Butyl-3-Methylimidazolium-Based Ionic Liquid Solvent Systems. *Green Chem.* **2010**, *12*, 268-275.

(50) Rosol, Z. P.; German, N. J.; Gross, S. M. Solubility, Ionic Conductivity and Viscosity of Lithium Salts in Room Temperature Ionic Liquids. *Green Chem.* **2009**, *11*, 1453-1457.
(51) Guhathakurta, S.; Min, K. Lithium Sulfonate Promoted Compatibilization in Single Ion Conducting Solid Polymer Electrolytes Based on Lithium Salt of Sulfonated Polysulfone and Polyether Epoxy. *Polymer* **2010**, *5*, 211-221.
(52) Bergman, R.; Börjesson, L.; Fytas, G.; Torell, L. M. Photon Correlation Study of Structural Relaxations in $NaCF_3SO_3$ Containing Polymer Electrolytes. *J. Non-Cryst. Solids* **1994**, *172-174*, 830-837.
(53) Mao, G.; R.F. Perea, W. S. H.; Price, D. L.; Saboungi, M.-L. Relaxation in Polymer Electrolytes on the Nanosecond Timescale. *Nature* **2000**, *405*, 163-165.
(54) Kubota, N.; Watanabe, H.; Konaka, G.; Eguchi, Y. Ionically Conductive Polymer Gel Electrolytes Prepared from Vinyl Acetate and Methyl Methacrylate for Electric Double Layer Capacitor. *J. Appl. Polym. Sci.* **2000**, *76*, 12-18.
(55) Meyer, F.; Sanz, G.; Eceiza, A.; Mondragon, I.; Mijović, J. The Effect of Stoichiometry and Thermal History During Cure on Structure and Properties of Epoxy Networks. *Polymer* **1995**, *36*, 1407-1414.
(56) Fernandez-Nograro, F.; Valea, A.; Llano-Ponte, R.; Mondragon, I. Dynamic and Mechanical Properties of DGEBA/Poly(Propylene Oxide) Amine Based Epoxy Resins as a Function of Stoichiometry. *Eur. Polym. J.* **1996**, *32*, 251-266.
(57) Hardwick, L. J.; Holzapfel, M.; Wokaun, A.; Novák, P. Raman Study of Lithium Coordination in EMI-TFSI Additive Systems as Lithium-Ion Battery Ionic Liquid Electrolytes. *J. Raman Spectrosc.* **2007**, *38*, 110-112.
(58) Le, M. L. P.; Cointeaux, L.; Strobel, P.; Leprêtre, J. C.; Judeinstein, P.; Alloin, F. Influence of Solvent Addition on the Properties of Ionic Liquids. *J. Phys. Chem. C* **2012**, *116*, 7712−7718.
(59) Parzuchowski, P. G.; Kiźlińska, M.; Rokicki, G. New Hyperbranched Polyether Containing Cyclic Carbonate Groups as a Toughening Agent for Epoxy Resin. *Polymer* **2007**, *48*, 1857-1865.

Table of Contents (TOC) Image

Composition as a Means to Control Morphology and Properties of Epoxy Based Dual-Phase Structural Electrolytes

Natasha Shirshova[*1], Alexander Bismarck[1,2], Emile S. Greenhalgh[3], Patrik Johansson[4], Gerhard Kalinka[5], Maciej J. Marczewski[4], Milo S.P. Shaffer[6], Malte Wienrich[5]